

Total-Variation Based Piecewise Affine Regularization

Jing Yuan¹, Christoph Schnörr¹, and Gabriele Steidl²

¹ Image and Pattern Analysis Group
Dept. Mathematics and Computer Science, University of Heidelberg, Germany
{yuanjing,schnoerr}@math.uni-heidelberg.de

² Appl. Math. Comp. Sci. Group
Dept. Mathematics and Computer Science, University of Mannheim
steidl@math.uni-mannheim.de

Abstract. We introduce a novel second-order regularizer, the Affine Total-Variation term, to capture the geometry of piecewise affine functions. The approach is characterized by two convex decompositions of a given image into piecewise affine structure and texture and noise, respectively. A convergent multiplier-based method is presented for computing a global optimum by computationally cheap iterative steps. Experiments with images and vector fields validate our approach and illustrate the difference to classical TV denoising and decomposition.

1 Introduction

1.1 Overview and Motivation

In this paper, we suggest and investigate a novel second-order regularization term,

$$\mathrm{TV}_a(u) := \int_{\Omega} \left(\sqrt{u_{xx}^2 + u_{yx}^2} + \sqrt{u_{xy}^2 + u_{yy}^2} \right) dx, \quad (1)$$

called *Affine Total Variation*, for denoising and decomposing functions into piecewise affine structures. Our work has been motivated by the basic total variation approach [15] to the *piecewise constant* regularization of functions, henceforth called *ROF-model*, and a recent extension of this approach suggested in [23] to the *piecewise harmonic* regularization of vector fields.

The latter approach demonstrates that by modifying the usual total variation term

$$\mathrm{TV}(u) = \int_{\Omega} |\nabla u| dx, \quad (2)$$

flows can be restored and decomposed into richer structure than merely piecewise constant functions, that only model a narrow subclass of real signals sufficiently accurate. At the same time, the basic structure of the ROF-model from the viewpoint of convex optimization has been preserved, such that standard methods from convex programming lead to efficient algorithms.

While the work [23] was motivated by flows related to image sequences from experimental fluid dynamics, our present work investigates *piecewise affine* regularization as an alternative to the piecewise harmonic case studied in [23]. Figure 1.1 shows the result of applying the novel regularizer (1) to a noisy image function. Our approach returns a denoised version of the input data with the piecewise affine structures preserved well. From the viewpoint of optimization, our approach has the same simple structure as the ROF-model. From the viewpoint of algorithm design, however, a bit more work is required to be able to resort to standard algorithms, due to the second-order partial derivatives appearing in (1).

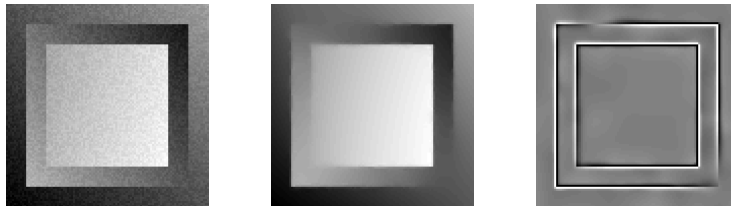


Fig. 1. From left to right. Noisy input image f , denoised image u using the regularizer (1), and the difference between the original noise-free image and the denoised image. Up to local errors at discontinuities, this latter image is almost constant which means that the piecewise affine structure underlying the noisy input data has been successfully restored.

1.2 Related Work and Contribution

Related work. Applying the standard TV-term (2) to general, not necessarily piecewise constant signals and images, leads to the well-known staircasing effect, that is to many jumps of the minimizing functions making the decomposition of the input data useless for signal interpretation. In this connection, higher-order regularization has been studied in the literature.

In [1], Chambolle and Lions propose an inf-convolution of the total-variation term and a functional based on the second-order derivatives:

$$R(u) = \min_{u=v+w} \int_{\Omega} |\nabla v| dx + \alpha \int_{\Omega} \left(\sqrt{w_{xx}^2 + w_{yx}^2 + w_{xy}^2 + w_{yy}^2} \right) dx.$$

A corresponding asymptotical case was studied in [16]. Chan et al. [3] adaptively add the Laplacian as regularizing term or replace the second summand in the inf-convolution by the Laplacian in [2] to avoid staircasing. After mollifying the TV-measure $\text{TV}(u) \approx \int_{\Omega} \sqrt{|\nabla u|^2 + \varepsilon} dx$, $\varepsilon \ll 1$, the corresponding Euler-Lagrange equation is iteratively solved by the lagged-diffusivity fixed-point method (cf. [19]). Likewise, You and Kaveh [20] and Didas et al. [5] investigate Laplacians Δu and variations thereof as argument of one convex functional. In

[11], Lysaker and Tai provide two regularizers

$$R_1(u) = \int_{\Omega} (|u_{xx}| + |u_{yy}|) dx \quad (3)$$

$$R_2(u) = \int_{\Omega} \sqrt{u_{xx}^2 + u_{yx}^2 + u_{xy}^2 + u_{yy}^2} dx \quad (4)$$

which are used in a PDE-based image diffusion process so as to avoid staircase effect in smooth regions and a fourth-order numerical scheme is given. In [12], Lysaker and Tai further introduce the convex combination of high-order regularizer and the classical total-variation term. The functional (3) was also considered in [8]. In [13], Rahman, Tai and Osher suggested a two-step high-order image denoising method, which first computes a denoised tangential field $\tau = (\tau_1, \tau_2)^t$, i.e. $\operatorname{div} \tau = 0$, by applying the regularizer $\int |\nabla \tau| dx$ which is actually equivalent to (4) for the image scalar field, then reconstructs the image gray-values by fitting the resulting normal field $n = (\tau_2, -\tau_1)$ through

$$\min_u \int_{\Omega} (|\nabla u| - \nabla u \cdot \frac{n}{|n|}) dx, \quad \text{s.t.} \quad \int_{\Omega} (u - f)^2 dx = \sigma^2.$$

Basically, the energy functionals used in our approaches possess the same structure as the work [11] except the applied nonsmooth high-order regularizer and the optimized functional proposed in (13b) is similar as the tangential-smoothing step suggested in [13] except that our approach tries to smooth the curl-free gradient field than the div-free field.

In connection with optical flow estimation, Trobin et al. [18] adopt from [4] the second-order term

$$t(u) := \frac{1}{\sqrt{3}} \left(\Delta u, \sqrt{2}(u_{xx} - u_{yy}), \sqrt{8}u_{xy} \right)^T,$$

and use the corresponding TV-term $\int_{\Omega} \sqrt{t(u) \cdot t(u)} dx$ for flow estimation. The derivation of $t(u)$ in [4] is based on Fourier transforms and motivated by designing local detectors for detecting ridges and valleys of image functions, say. As a consequence, the corresponding TV-term appears not to be a proper basis for piecewise affine decomposition, and boundaries are not treated adequately (as is clearly visible e.g. in Fig. 2f in [18]).

Contribution. Our contribution consists in devising a novel regularization term (1) that provides a mathematically precise solution to the problem of denoising piecewise affine signals. Staircasing is suppressed as well, and an augmented Lagrangian based problem decomposition is derived that enables to compute a global optimum by iterating computationally simple iterative steps. Numerical experiments are presented mainly to illustrate and validate properties of the approach.

2 Subspaces and Orthogonal Decompositions

Let $\Omega \subset \mathbb{R}^2$ be an open bounded and simply-connected domain with Lipschitz-continuous boundary $\partial\Omega$. For scalar-valued functions, we denote by $|\cdot|_p, 1 \leq p <$

∞ the usual $L_p(\Omega)$ norm and by $\langle \cdot \rangle$ the $L_2(\Omega)$ inner product. For vector-valued functions $g = (g_1, g_2)^\top$, we set $\|g\|_p := \|\sqrt{g_1^2 + g_2^2}\|_p$ and $\langle g, h \rangle_\Omega := \langle g_1, h_1 \rangle + \langle g_2, h_2 \rangle$. Further, we use the notation $\bar{u} := |\Omega|^{-1} \int_\Omega u \, dx$ for the average of u and $\nabla u := (u_x, u_y)^\top$, $\nabla^\perp u := (u_y, -u_x)^\top$, $\operatorname{div} g := g_{1x} + g_{2y}$ and $\operatorname{curl} g := g_{1y} - g_{2x}$. Let $H^1(\Omega)$ denote the Sobolev spaces with the inner product

$$\langle u, v \rangle_{H^1} := \langle \nabla u, \nabla v \rangle_\Omega + \bar{u} \bar{v} \quad (5)$$

and let $H_0^1(\Omega) := \{u \in H^1(\Omega) : u|_{\partial\Omega} = 0\}$. We are interested in the space

$$H(\Omega) := \{u \in H^1(\Omega) : \partial_n u|_{\partial\Omega} = (\bar{u}_x, \bar{u}_y)^\top \cdot n\},$$

where n denotes the outer unit normal vector at the boundary $\partial\Omega$. By the following proposition, we can decompose functions $u \in H(\Omega)$ into a globally affine component u_a and an oscillating part u_o .

Proposition 1. *The space $H(\Omega)$ admits the orthogonal decomposition*

$$H(\Omega) = H_a(\Omega) \oplus_{H^1} H_o, \quad (6a)$$

$$H_a(\Omega) := \{u \in H(\Omega) : \nabla u = (\bar{u}_x, \bar{u}_y)^\top\}, \quad (6b)$$

$$H_o(\Omega) := \{u \in H(\Omega) : \bar{u} = \bar{u}_x = \bar{u}_y = 0, \partial_n u|_{\partial\Omega} = 0\}. \quad (6c)$$

Proof. For any $u \in H(\Omega)$, let $u_{ox} := u_x - \bar{u}_x$ and $u_{oy} := u_y - \bar{u}_y$. Then $u_a := \bar{u}_x x + \bar{u}_y y + \bar{u} \in H_a(\Omega)$ and the function u_o defined by its partial derivatives u_{ox} , u_{oy} and by $\bar{u}_o = 0$ belongs to $H_o(\Omega)$. Moreover, we have that $u = u_a + u_o$. The orthogonality of the decomposition follows by

$$\langle u_a, u_o \rangle_{H^1} = \langle \nabla u_a, \nabla u_o \rangle_\Omega + \bar{u}_a \bar{u}_o = \bar{u}_x \int_\Omega u_{ox} \, dx + \bar{u}_y \int_\Omega u_{oy} \, dx = 0. \quad \square$$

The Helmholtz decomposition of vector fields, see [6, 21, 22] also for the discrete setting, is given by

$$L_2(\Omega)^2 = \nabla H^1(\Omega) \oplus \nabla^\perp H_0^1(\Omega),$$

where the spaces can be also characterized by $\nabla H^1(\Omega) = \{v \in L_2(\Omega)^2 : \operatorname{curl} v = 0\}$ and $\nabla^\perp H_0^1(\Omega) = \{v \in L_2(\Omega)^2 : \operatorname{div} v = 0, v \cdot n|_{\partial\Omega} = 0\}$. We will need the space

$$V(\Omega) := \{v \in L_2(\Omega)^2 : v \cdot n|_{\partial\Omega} = 0, \bar{v}_1 = \bar{v}_2 = 0\}. \quad (7)$$

By the Helmholtz decomposition, this space admits the orthogonal decomposition

$$V(\Omega) = V_\nabla(\Omega) \oplus V_{\nabla^\perp}(\Omega), \quad (8)$$

where $V_\nabla(\Omega) := \{v \in \nabla H^1(\Omega) : v \cdot n|_{\partial\Omega} = 0, \bar{v}_1 = \bar{v}_2 = 0\}$ and $V_{\nabla^\perp}(\Omega) := \{v \in \nabla^\perp H_0^1(\Omega) : \bar{v}_1 = \bar{v}_2 = 0\}$.

Proposition 2. *For every vector field $v \in V_\nabla(\Omega)$, there is a unique function $u_o \in H_o(\Omega)$ with $v = \nabla u_o$.*

Proof. By definition we have for any $v \in V_{\nabla}(\Omega)$ that there exists $u \in H^1(\Omega)$ such that $v = \nabla u$. Then we see that $v \cdot n|_{\partial\Omega} = \partial_n u|_{\partial\Omega} = 0$ and $\bar{v}_1 = \bar{u}_x = 0$, $\bar{v}_2 = \bar{u}_y = 0$. On the other hand, $u_o \in H_o$ is uniquely determined by the Neumann problem

$$\Delta u_o = \operatorname{div} v, \quad \partial_n u_o|_{\Omega} = 0, \quad \bar{u}_o = 0. \quad \square \quad (9)$$

3 Variational Approaches

In the rest of this paper, we follow the *first discretize, then optimize* paradigm, yet adopt the usual (continuous) notation that is easier to read. Accordingly, all operators like $\nabla, \operatorname{div}$ etc. denote linear mappings between finite dimensional spaces, $|\cdot|_p$ are the usual ℓ_p norms and for $g := (g_i)_{i=1}^n$, $g_i \in \mathbb{R}^2$ $\|g\|_p := (|g_i|_2)_{i=1}^n|_p$. In the following, we denote by δ_C the indicator function of a convex set C , i.e. $\delta_C(x) := 0$ if $x \in C$, and $\delta_C(x) := \infty$ otherwise and by P_C the orthogonal projector onto C .

We exhibit the effect of the regularizer (1) by computing a dual representations of the optimization problems (13) in accordance to the dual formulation of the ROF-model.

In general, if $g : \mathbb{R}^n \rightarrow \mathbb{R}$ and $\Phi : \mathbb{R}^m \rightarrow \mathbb{R}$ are proper, closed convex functions and $D : \mathbb{R}^n \rightarrow \mathbb{R}^m$ is a linear operator, then the following problem (P) has the dual (D):

$$(P) \quad \inf_{u \in \mathbb{R}^n} \{g(u) + \Phi(Du)\}, \quad (D) \quad - \inf_{p \in \mathbb{R}^m} \{g^*(-D^*p) + \Phi^*(p)\},$$

where g^* denotes the conjugate function of g . For the problems considered in the following, it can be shown that solutions of the primal and dual problem exist and that the duality gap is zero.

Rudin-Osher-Fatemi (ROF) Model. We recall some basic formulas as a reference for our approach presented below. The ROF-model reads

$$\inf_u \left\{ \frac{1}{2} |f - u|_2^2 + \alpha \operatorname{TV}(u) \right\}, \quad \alpha \operatorname{TV}(u) := \sigma_{C_\alpha}(u), \quad (10)$$

where $C_\alpha := \operatorname{div} B_\alpha$, $B_\alpha := \{p : \|p\|_\infty \leq \alpha\}$.

Let \hat{u} denote the minimizer of (10). Setting $g(u) := \frac{1}{2} |f - u|_2^2$, $D := I$ and $\Phi(u) := \alpha \operatorname{TV}(u)$ and regarding that $g^*(v) := \frac{1}{2} |f + v|_2^2 - \frac{1}{2} |f|^2$ and $\Phi^*(v) = \delta_{C_\alpha}$ the dual problem reads

$$- \inf_{v \in C_\alpha} \left\{ \frac{1}{2} |f - v|_2^2 - \frac{1}{2} |f|^2 \right\}, \quad (11)$$

where we have replaced v by $-v$ by the symmetry of C_α . Consequently, if

$$\hat{p} := \operatorname{argmin}_{p \in B_\alpha} \left\{ \frac{1}{2} |f - \operatorname{div} p|_2^2 \right\} \quad (12)$$

then $\hat{v} := \operatorname{div} \hat{p} = P_{C_\alpha}(f)$ is the minimizer of the dual problem. Primal and dual solutions are related by the optimality condition $f - \operatorname{div} \hat{p} = \hat{u}$, that in turn yields the image decomposition $f = \hat{u} + \hat{v}$.

Affine Variational Models. Based on the regularizer (1) we consider two variational approaches:

$$\inf_u \left\{ \frac{1}{2} |u - f|_2^2 + \alpha \operatorname{TV}_a(u) \right\}, \quad (13a)$$

$$\inf_u \left\{ \frac{1}{2} |u - f|_{H^1}^2 + \alpha \operatorname{TV}_a(u) \right\}. \quad (13b)$$

These approaches differ due to the data term which is the usual one in case of (13a), whereas the data term in (13b) is induced by the discrete counterpart of the inner product (5).

3.1 Variational Approach (13a)

We introduce an auxiliary vector field v in order to express the regularizer (1) in term of the ordinary TV-measure defined in (2). Then approach (13a) reads

$$\inf_{u,v} \left\{ \frac{1}{2} |f - u|_2^2 + \alpha \operatorname{TV}(v_1) + \alpha \operatorname{TV}(v_2) \right\}, \quad \text{subject to } v = \nabla u. \quad (14)$$

i.e.,

$$\inf_{u,v} \left\{ \{g(u, v) + \Phi(D(u, v)^T)\} \right\}$$

with $g(u, v) := \frac{1}{2} |f - u|_2^2 + \alpha \operatorname{TV}(v_1) + \alpha \operatorname{TV}(v_2)$, $\Phi := \delta_0$, $D := (\nabla \ - I)$. Since $g^*(r, s) = \frac{1}{2} |f + r|_2^2 - \frac{1}{2} |f|^2 + \delta_{C_\alpha}(s_1) + \delta_{C_\alpha}(s_2)$, $\Phi^* \equiv 0$ and $-D^* = \begin{pmatrix} \operatorname{div} \\ I \end{pmatrix}$ the dual problem becomes

$$- \inf_{q \in C_\alpha^2} \left\{ g^* \left(\begin{pmatrix} \operatorname{div} \\ I \end{pmatrix} q \right) \right\} = - \inf_{q \in C_\alpha^2} \left\{ \frac{1}{2} |f - \operatorname{div} q|_2^2 - \frac{1}{2} |f|^2 \right\}.$$

This formulation parallels the dual formulation (11) of the ROF-model. Let

$$\hat{q} := \operatorname{argmin}_{q \in C_\alpha^2} \frac{1}{2} |f - \operatorname{div} q|_2^2. \quad (15)$$

The higher-order TV regularization becomes apparent through the texture part of f which is defined by the orthogonal projection $\hat{v} = \operatorname{div} \hat{q} = P_{\operatorname{div} C_\alpha^2}(f)$ onto a different convex set.

An alternative, more explicit characterization of the regularization effect of (1) in terms of the auxiliary field $v = \nabla u$ is obtained by reformulating (13a) as

$$\inf_v \left\{ G(v) + \alpha (\operatorname{TV}(v_1) + \operatorname{TV}(v_2)) \right\}, \quad \text{where } G(v) := \inf_{u, \nabla u = v} \frac{1}{2} |u - f|_2^2 \quad (16)$$

Exploiting strong duality again we obtain that

$$G(v) = -\inf_p \left\{ \frac{1}{2} \|f - \operatorname{div} p\|_2^2 - \frac{1}{2} \|f\|_2^2 - \langle v, p \rangle_\Omega \right\}. \quad (17)$$

Fermat's rule yields that the minimizer \hat{p} has to fulfill $\nabla \operatorname{div} \hat{p} = \nabla f - v$ and, in turn, $\Delta(\operatorname{div} \hat{p}) = \Delta f - \operatorname{div} v$. Insertion into $G(v)$ in (17) yields for (16) (omitting the constant)

$$\inf_v \left\{ \frac{1}{2} \|\Delta^{-1}(\Delta f - \operatorname{div} v)\|_2^2 + \alpha(\operatorname{TV}(v_1) + \operatorname{TV}(v_2)) \right\} \quad (18)$$

This representation of (13a) and (15), respectively, shows that the edge image Δf is approximated by the divergence of a piecewise smooth vector field v in terms of the $|\cdot|_{\Delta^{-2}}$ -norm. Clearly, inserting $v = \nabla u$ into $\Delta^{-1}(\Delta f - \operatorname{div} v)$ yields $\frac{1}{2} \|f - u\|_2^2$ from (13a).

3.2 Variational Approach (13b)

The data term of problem (13b) decomposes according to the orthogonal decomposition (6a). By construction, the affine component u_a of $u = u_a + u_o$ is not affected by the regularizer. Thus, $\hat{u}_a = f_a$, where f_a can be computed in a preprocessing step. It remains to minimize

$$\inf_{u_o, v} \left\{ \frac{1}{2} \|\nabla f_o - v\|_2^2 + \alpha(\operatorname{TV}(v_1) + \operatorname{TV}(v_2)) \right\}, \quad \text{subject to } v = \nabla u_o.$$

Due to the Prop. 2 the linear constraint can be expressed as $\delta_{V_\nabla}(v)$. Reasoning similar to the previous section yields

$$\begin{aligned} & \sup_w \left\{ \langle w, \nabla f_o - v \rangle_\Omega - \frac{1}{2} \|w\|_2^2 \right\} + \sup_{q \in C_\alpha^2} \langle q, -v \rangle_\Omega + \delta_{V_\nabla}(v) \\ &= \sup_{w, q \in C_\alpha^2} \left\{ \langle w + q, -v \rangle_\Omega + \delta_{V_\nabla}(v) + \langle w, \nabla f \rangle_\Omega - \frac{1}{2} \|w\|_2^2 \right\} \end{aligned}$$

Interchanging inf and sup and taking \inf_v (ignoring constants), we obtain

$$\inf_{w, q \in C_\alpha^2} \frac{1}{2} \|\nabla f_o - w\|_2^2 \quad \text{subject to } w + q \in V_{\nabla^\perp}. \quad (19)$$

The minimizer \bar{w} is obviously an element of V_∇ , which together with the constraints $q \in C_\alpha^2$, $w + q \in V_{\nabla^\perp}$ leads to the reformulation of (19)

$$\inf_{q \in P_\nabla(C_\alpha^2)} \frac{1}{2} \|\nabla f_o - q\|_2^2. \quad (20)$$

Here P_∇ denotes the orthogonal projector onto the subspace V_∇ . To compare this approach with (15), we rewrite (20) as

$$\inf_{q \in P_\nabla(C_\alpha^2)} \frac{1}{2} \|\nabla(f_o - \Delta^{-1} \operatorname{div} q)\|_2^2 = \inf_{q \in P_\nabla(C_\alpha^2)} \frac{1}{2} \|\nabla(\Delta^{-1}(\Delta f_o - \operatorname{div} q))\|_2^2, \quad (21)$$

where Δ^{-1} stands for the solution operator of problem (9). Approach (15), on the other hand, is given by

$$\inf_{q \in C_\alpha^2} |f_a + (f_o - \operatorname{div} q)|_2^2. \quad (22)$$

Taking into account the representation of vector fields $q \in V_\nabla$ by a potential functions ϕ_q in terms of $q = \nabla \phi_q$ viz. $\operatorname{div} q = \Delta \phi_q$ (Prop. 2), we see that (21) focuses on the decomposition of the edge set Δf , whereas (22) decomposes f and does not discriminate the two components f_a and f_o .

Comparing (21) on the other hand with (18) indicates how regularization of the large-scale structural components of f is accomplished by (21) in terms of the small-scale texture component ϕ_q , by taking the gradient (after smoothing with Δ^{-1}) and projection onto a suitable set $P_\nabla(C_\alpha^2)$.

4 Optimization

In this section we specify algorithms for computing a global minimum of (13a) and (13b), respectively. We apply an alternating version of the split Bregman algorithm [7]. Note that the split Bregman algorithm coincides with the augmented Lagrangian method applied to the primal problem [14] and that its alternating version is just a Douglas-Rachford splitting for the dual problem [17]. The convergence properties of this technique are well known.

4.1 Algorithm Minimizing (13a)

The split Bregman algorithm for (14) reads

$$\begin{aligned} (u^{(k+1)}, v^{(k+1)}) &= \operatorname{argmin}_{u,v} \left\{ \frac{1}{2} |f - u|_2^2 + \alpha(\operatorname{TV}(v_1) + \operatorname{TV}(v_2)) \right. \\ &\quad \left. + \frac{1}{2\tau} \|\nabla u - v\|_2^2 + \langle b^{(k)}, \nabla u - v \rangle_\Omega \right\}, \\ b^{(k+1)} &= b^{(k)} + \frac{1}{\tau} (\nabla u^{(k+1)} - v^{(k+1)}). \end{aligned}$$

Alternating the minimization of $u^{(k+1)}$ and $v^{(k+1)}$ we obtain

$$\begin{aligned} v^{(k+1)} &= \operatorname{argmin}_v \left\{ \alpha(\operatorname{TV}(v_1) + \operatorname{TV}(v_2)) + \frac{1}{2\tau} \|\nabla u^{(k)} + \tau b^{(k)} - v\|_2^2 \right\}, \\ u^{(k+1)} &= \operatorname{argmin}_u \left\{ \frac{1}{2} |f - u|_2^2 + \frac{1}{2\tau} \|\nabla u + \tau b^{(k)} - v^{(k+1)}\|_2^2 \right\}. \end{aligned}$$

Then $v^{(k+1)}$ follows as in the ROF approach by

$$v^{(k+1)} = \nabla u^{(k)} + \tau b^{(k)} - P_{C_{\alpha\tau}^2}(\nabla u^{(k)} + \tau b^{(k)})$$

and $u^{(k+1)}$ can be computed by setting the gradient to zero

$$u^{(k+1)} = (I - \frac{1}{\tau} \Delta)^{-1} (f - \operatorname{div}(\frac{1}{\tau} v^{(k+1)} - b^{(k)}))$$

Algorithm. Initialization: $b^{(0)} = 0$ and $u^{(0)} = f$
For $k = 0, 1, \dots$ iterate until a convergence criterion is reached

$$\begin{aligned} w^{(k+1)} &:= \nabla u^{(k)} + \tau b^{(k)} \\ v^{(k+1)} &:= w^{(k+1)} - P_{C_{\alpha\tau}^2}(w^{(k+1)}) \\ u^{(k+1)} &:= (I - \frac{1}{\tau}\Delta)^{-1}(f - \operatorname{div}(\frac{1}{\tau}v^{(k+1)} - b^{(k)})) \\ b^{(k+1)} &:= b^{(k)} + \frac{1}{\tau}(\nabla u^{(k+1)} - v^{(k+1)}) \end{aligned}$$

4.2 Algorithm Minimizing (13b)

Based on the derivation in section 3.2, we consider

$$\inf_{u_o, v} \left\{ \frac{1}{2} \|\nabla f_o - \nabla u_o\|_2^2 + \alpha(\operatorname{TV}(v_1) + \operatorname{TV}(v_2)) \right\}, \quad \text{subject to } v = \nabla u_o.$$

and have to iterate

$$\begin{aligned} (u^{(k+1)}, v^{(k+1)}) &= \operatorname{argmin}_{u, v} \left\{ \frac{1}{2} \|\nabla f_o - \nabla u\|_2^2 + \alpha(\operatorname{TV}(v_1) + \operatorname{TV}(v_2)) \right. \\ &\quad \left. + \frac{1}{2\tau} \|\nabla u - v\|_2^2 + \langle b^{(k)}, \nabla u - v \rangle_{\Omega} \right\}, \\ b^{(k+1)} &= b^{(k)} + \frac{1}{\tau}(\nabla u^{(k+1)} - v^{(k+1)}). \end{aligned}$$

Alternating the first minimization process we obtain the following algorithm

Algorithm. Initialization: $b^{(0)} = 0$ and $u^{(0)} = f$
For $k = 0, 1, \dots$ iterate until a convergence criterion is reached

$$\begin{aligned} w^{(k+1)} &:= \nabla u^{(k)} + \tau b^{(k)} \\ v^{(k+1)} &:= w^{(k+1)} - P_{C_{\alpha\tau}^2}(w^{(k+1)}) \\ u^{(k+1)} &:= \frac{\tau}{1+\tau} \Delta^{-1} \operatorname{div}(\nabla f_o + (\frac{1}{\tau}v^{(k+1)} - b^{(k)})) \\ b^{(k+1)} &:= b^{(k)} + \frac{1}{\tau}(\nabla u^{(k+1)} - v^{(k+1)}) \end{aligned}$$

5 Numerical Experiments

In this section we illustrate the properties of our approach with few numerical experiments. The mimetic finite difference method [9, 10] is used for discretizing relevant scalar fields and vector fields and a detailed implementation of the nonlinear functionals is given in [22]. By this numerical scheme, the relevant boundary conditions are kept well and turn out to be compatible with the corresponding integral identities.

Signals. Figure 2 shows that our approach (13b) effectively removes noise without staircasing effect, in contrast to the ROF model. We also point out that boundaries are treated without introducing artifacts.

Variational approach (13a) versus (13b). Figure 3 compares the minimizers of the two variational approaches (13a) and (13b) for an arbitrary image section.

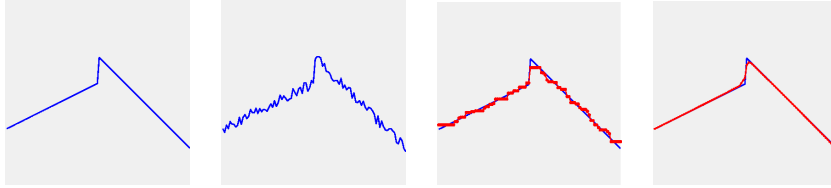


Fig. 2. Ground truth and noisy input data are shown by the first two graphs respectively. Standard TV-regularization (ROF model) leads to the well-known staircasing effect (see 3rd. picture). Piecewise affine TV regularization effectively removes noise and recovers the piecewise affine signal structure (see 4th picture).

The last two pictures of Figure 3 depict 3D plots of the minimizers subtracted from the original image section. The plot on 5th graph corresponding to the approach (13b) clearly indicates an approximation “error” that is not noticeable in the plot on 4th graph corresponding to (13a). This result confirms the discussion above of formal differences between equations (21) and (22) and the $|\cdot|_{H_1}^2$ based data term is more sensitive to large noises due to the noise amplification by partial derivatives.



Fig. 3. From left to right. Original image section, minimizer of (13a), minimizer of (13b), 3D plots of the minimizers subtracted from the original data illustrate a major difference between the variational approaches (13a) and (13b). While the 4th plot on the shows almost pure noise, the rightmost plot indicates an estimation error due to using the $|\cdot|_{H_1}^2$ data term which is sensitive to large noise levels.

Denosing of vector fields. Figure 4 compares the standard TV regularization (ROF model) with piecewise affine TV regularization for the denosing of vector fields. The input data simulate estimates obtained for a moving camera in a scene with moving objects. This scenario is roughly represented by a piecewise planar layout of the scene. The numerical results confirm again that our approach returns useful estimates of both denoised vector fields and its discontinuities, while the ROF-model only returns discontinuities but no useful vector field estimates.

6 Conclusion

We presented a novel convex variational approach to the denosing and the decomposition of signals, images and vector fields. Based on a suitable orthogonal decomposition of the underlying vector space, a TV measure comprising second-order derivatives was introduced that enables to denoise noisy input data and

to preserve piecewise affine signal structure using standard algorithms of convex programming. The latter are computationally simple due to a problem decomposition employing the augmented Lagrangian and primal and dual variables. By deriving dual variational formulations akin to the ROF model, differences between first- and second order regularization and between two alternative data terms were worked out. Numerical experiments confirm these findings.

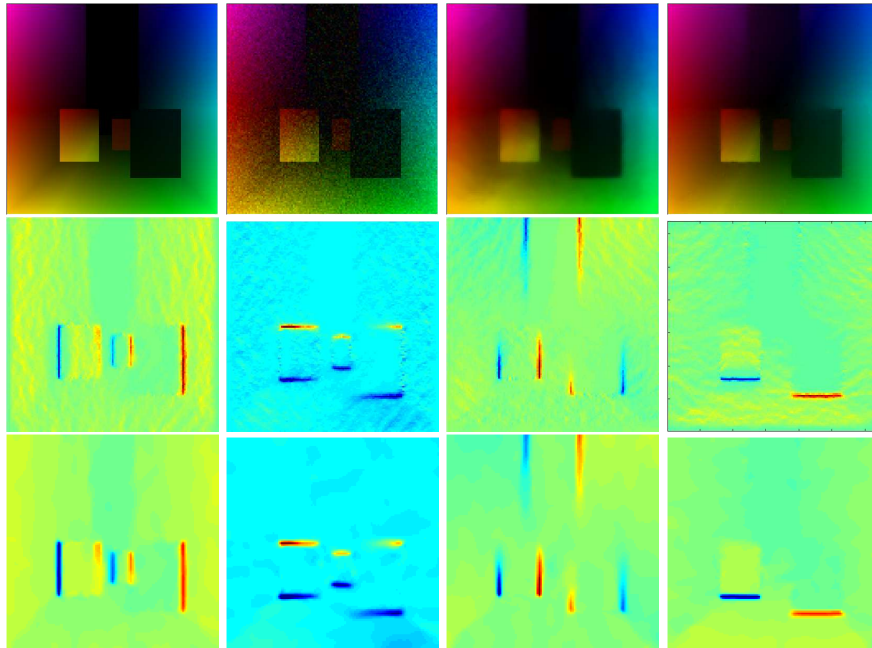


Fig. 4. Top. Color-coded motion field corresponding to a moving camera and static as well as moving objects represented by sections of planes; ground-truth (1st. fig.), input data (2nd. fig.), the ROF-based result (3rd. fig.) and the affine regularization-based (13a) result (4th. fig.) . **Last two rows:** Components of ∇u_1 and ∇u_2 for the ROF model (2nd. row) and for piecewise affine regularization (3rd. row). The result on the right illustrates that through piecewise affine regularization no staircasing effect occurs, thus enabling both discontinuity detection and motion estimation, while the latter is not feasible for such scenarios with the standard ROF-model.

References

1. A. Chambolle and P.-L. Lions. Image recovery via total variation minimization and related problems. *Numer. Math.*, 76(2):167–188, 1997.
2. T. Chan, S. Esedoglu, and F. E. Park. Image decomposition combining staircase reduction and texture extraction. *J. Visual Communication and Image Representation*, 18(6):468–486, 2007.

3. T. Chan, A. Marquina, and P. Mulet. Higher-order total variation-based image restoration. *SIAM J. Sci. Comput.*, 22(2):503–516, 2000.
4. P. E. Danielsson and Q. Lin. Efficient detection of second-degree variations in 2d and 3d images. *J. Vis. Comm. Image Repr.*, 12:255–305, 2001.
5. S. Didas, S. Setzer, and G. Steidl. Combined ℓ_2 data and gradient fitting in conjunction with ℓ_1 regularization. *Advances in Computational Mathematics*, 30(1):79–99, 2009.
6. V. Girault and P.-A. Raviart. *Finite Element Methods for Navier-Stokes Equations*. Springer, 1986.
7. D. Goldstein and S. Osher. The Split Bregman method for l_1 regularized problems. UCLA CAM Report, 2008.
8. W. Hintermüller and K. Kunisch. Total bounded variation regularization as a bilaterally constraint optimization problem. *SIAM J. Appl. Math.*, 64(4):1311–1333, 2004.
9. J. M. Hyman and M. Shashkov. Natural discretizations for the divergence, gradient, and curl on logically rectangular grids. *Comput. Math. Appl.*, 33(4):81–104, 1997.
10. James M. Hyman and Mikhail Shashkov. Adjoint operators for the natural discretizations of the divergence, gradient and curl on logically rectangular grids. *Appl. Numer. Math.*, 25(4):413–442, 1997.
11. M. Lysaker, A. Lundervold, and X. C. Tai. Noise removal using fourth-order partial differential equation with applications to medical magnetic resonance images in space and time. *IEEE Trans. Image Processing*, 12(12):1579–1590, December 2003.
12. M. Lysaker and X. C. Tai. Iterative image restoration combining total variation minimization and a second-order functional. *International Journal of Computer Vision*, 66(1):5–18, January 2006.
13. T. Rahman, X. C. Tai, and S. J. Osher. A TV-stokes denoising algorithm. In *Scale-Space*, volume 4485 of *LNCS*, pages 473–483, 2007.
14. R.T. Rockafellar. Augmented Lagrangians and applications of the proximal point algorithm in convex programming. *Math. Oper. Res.*, 1(2):97–116, 1976.
15. L. Rudin, S. Osher, and E. Fatemi. Nonlinear total variation based noise removal algorithms. *Physica D*, 60:259–268, 1992.
16. O. Scherzer. Denoising with higher order derivatives of bounded variation and an application to parameter estimation. *Computing*, 60:1–27, 1998.
17. S. Setzer. Split Bregman algorithm, Douglas-Rachford splitting and frame shrinkage. In K. A. Lie, M Lysaker, K. Morken, and X.-C. Tai, editors, *Scale Space and Variational Methods*, LNCS. Springer, 2009.
18. W. Trobin, T. Pock, D. Cremers, and H. Bischof. An unbiased second-order prior for high-accuracy motion estimation. In G. Rigoll, editor, *DAGM 2008*, volume 5096 of *LNCS*, pages 296–405. Springer, 2008.
19. C. R. Vogel. *Computational Methods for Inverse Problems*. SIAM, 2002.
20. Y. L. You and M. Kaveh. Fourth-order partial differential equations for noise removal. *IEEE Trans. Image Processing*, 9(10):1723–1730, October 2000.
21. J. Yuan, C. Schnörr, and Memin E. Discrete orthogonal decomposition and variational fluid flow estimation. *J. Math. Imaging and Vision*, 28(1):67–80, May 2007.
22. J. Yuan, C. Schnörr, and G. Steidl. Simultaneous optical flow estimation and decomposition. *SIAM J. Scientific Computing*, 29(6):2283–2304, 2007.
23. J. Yuan, C. Schnörr, and G. Steidl. Convex hodge decomposition and regularization of image flows. *J. Math. Imag. Vision*, 33(2):169–177, 2009.